KAAN Technology Club
SUAS 2026
Technical Design Report

Abstract—**This document presents the Technical Design Report for the KAAN Technology Club's unmanned aerial vehicle (UAV) developed for the SUAS 2026 competition. To fulfill complex mission requirements under strict size, weight, and operational constraints, a custom quadrotor platform was selected and optimized. The system integrates a Pixhawk Orange Cube flight controller for autonomous navigation and a Raspberry Pi 5 companion computer for mission execution. The mission system utilizes a fine-tuned RF-DETR deep learning model for real-time target detection and geodesic localization, a specialized dual-pulley servo-driven payload release mechanism with rotary damping for precision delivery, and OpenDroneMap for high-efficiency photogrammetry. Structural integrity and propulsion feasibility were validated through ANSYS finite element analysis and Gazebo software-in-the-loop simulations. Contingency strategies, including edge AI fallback via a Hailo-8 HAT and manual detection protocols, ensure high operational reliability under challenging field conditions.**

Index Terms—**Unmanned Aerial Vehicles (UAV), Autonomous Delivery, Object Detection, RF-DETR, Photogrammetry, OpenDroneMap, System Integration.**

ACKNOWLEDGMENT

The KAAN Technology Club sincerely thanks the Republic of Türkiye Ministry of Youth and Sports (GSB) for their vital sponsorship and support. We also extend our gratitude to our university advisors, lab coordinators, and industry partners for their guidance and contributions to the development of our UAV platform for the SUAS 2026 competition.

I. COMPETITION STRATEGY

The first challenge we faced when defining our strategic vision was deciding which UAV platform to choose. Based on the experience our team has gained over the years, we determined that a VTOL was the most suitable platform for this competition. The reason for this is that VTOLs offer not only long flight times but also the ability to perform precision object delivery. However, since most team members are fourth-year students, their course loads are heavy, and developing a system of this complexity did not seem realistic. As a result, we decided to use a rotary-wing platform for the competition, which has a simpler design but can still fulfill most of the mission requirements. This allowed us to upgrade the rotary-wing platform we used in last year's SUAS competition and dedicate the remaining time to successfully executing the updated mission scenario.

The platform's rotary-wing design brought with it several advantages and disadvantages. It became easier to bring the vehicle's weight closer to the maximum allowed of 15 lbs. At the same time, by making the vehicle smaller, it became possible to fit it into a carry-on suitcase. However, since rotary-wing aircraft have limited speed and flight duration, calculations revealed that the vehicle could not exceed four laps in the flight endurance mission. When the drone's speed is calculated at 10 m/s, a 2-mile lap is completed in approximately 5 minutes and 22 seconds, while four laps exceed 20 minutes. In this scenario, it yields 32 points out of a possible 200, leaving no time for the other tasks. Ultimately, the decision was made to abandon the flight endurance task in order to complete the other tasks.

In addition, battery packs will be reduced to less than 100 Wh, which will also earn full points. Tool-less assembly, however, will not be possible due to the unavailability of the necessary parts.

Since abandoning the flight endurance mission cost the team nearly 200 points, the goal was to fully complete all other missions. First, it was decided that there would be two operators during the mission. In this scenario, both mapping and delivery must be fully autonomous.

The general mission will be carried out through the steps illustrated in Fig. 1. When the mission begins, the drone will start autonomously following the flight path preloaded into its system. After completing one lap along the designated route, it will begin flying in a zigzag pattern over the search area. During this process, it will take regular photographs of the ground. The captured images will be transmitted to the ground station in real time. Artificial intelligence algorithms will be run on each photo taken to detect the locations of objects. Once the area has been scanned, the ground station will begin creating a map using the photos. While the map-building process continues, the drone will drop payloads onto the objects it has detected. After the delivery is complete, the drone will switch to RTL mode and conclude the mission. The remainder of the time will be spent waiting for the map to be generated. Since map generation takes a long time, the drone's landing must occur at least 20 minutes after the mission end time. Overall, the drone will take the photos and initiate RTL within 25 minutes; the remaining time will be spent waiting.

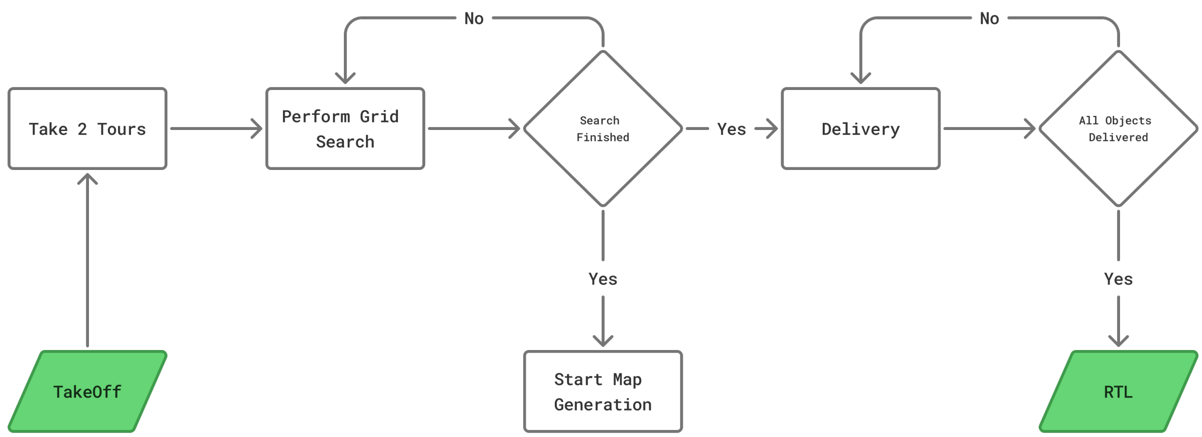

Fig. 1. Competition Flowchart

II. Design Strategy

The system design for this project is divided into two parts as shown in Fig. 2: the Flight System and the Mission System. The Flight System is the combination of systems necessary for flight found in any drone. Basic functions such as the drone's takeoff, movement, pilot-controlled operation, and autonomous flight are included in this system. The Mission System, on the other hand, is a system that can intervene in the Flight System to perform the tasks assigned in the competition. It includes systems that enable the drone to take photographs, process these photographs using artificial intelligence, and deploy a payload. The central component of the Flight System is the Pixhawk Orange Cube, while the central component of the Mission System is the Raspberry Pi. These two components are connected via the MAVLink [MAV23] protocol.

Fig. 2. Flight System and Mission System

A. *Flight Control System and Structural Design*

The **Pixhawk Orange Cube** [Hex20] flight control board, which is the central component of the flight system, enables the drone to fly autonomously. The **Here4 GPS** [Hex21] module was used to calculate object positions and determine the drone's position relative to the Earth. To allow the drone to be controlled by a pilot, the **R12DS** receiver and the **AT12** controller were used. The **rfd900x** telemetry system was chosen to enable the loading of missions and the real-time monitoring of vital drone data such as speed, altitude, and position.

*1) **Structure**:*

*a) **Requirements**:* The primary objective of the SUAS 2026 platform is to provide an aerial system capable of reliable and autonomous operations while adhering to the size, weight, and operational constraints specified by the competition. Fllowing Table. I shows requirements analysis.

Competition Requirements	Design Requirements
The UAV must comply with volume restrictions	Target Volume (22 x 14 x 9 in)
Autonomous mission execution	A companion computer is required
Payload delivery	Specialized mission mechanism
Reliable object detection	Fixed-mount camera platform

TABLE I
Structure Requirements Analysis

*b) **Concept Selection**:* In Table. II comparative analysis was conducted for the concept to be selected in accordance with the competition requirements.

Based on the analysis, the quadrotor concept that received the highest score in terms of high flight stability, ease of payload installation, structural simplicity, low development risk, and flight durability was selected as the one that meets the competition requirements.

*c) **Material Selection**:* Carbon fiber was selected as the primary structural material due to its superior strength-to-weight ratio compared to aluminum and traditional 3D-

Criterion	Weight	HTOL	VTOL	Quad
Hovering Stability	30%	2	4	5
Payload Delivery	20%	2	4	5
Structural Simplicity	20%	2	2	4
Development Risk	15%	4	2	5
Flight Durability	15%	3	5	3
Total Score		2.45	3.45	4.5

TABLE II
CONCEPT SELECTION

printed materials, its low density, and its corrosion resistance. Comparison between alternatives shown in Table. III.

Property	Carbon Fiber	Aluminum 6061
Density (kg/m³)	1600	2700
Specific Strength	High	Medium
Corrosion Resistance	Excellent	Good

TABLE III
MATERIAL SELECTION

*d) **Airframe Design**:* The UAV system features a rigid structure consisting of CNC-machined carbon fiber center plates and carbon fiber arms integrated into these plates. This structure provides high strength combined with low weight, creating a platform that maintains flight stability while safely carrying mission payloads.

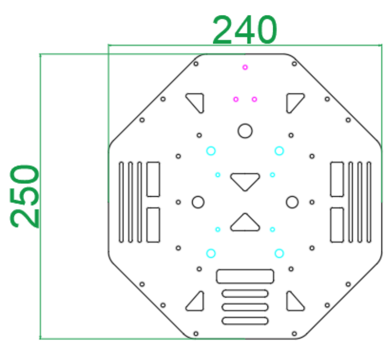

Fig. 3. Airframe Base

The central carbon fiber panels were specially designed by the team to meet competition requirements and are configured to optimize the layout of the subsystems. This has resulted in both a balanced weight distribution and an efficient architecture in terms of system integration. Fig. 3 shows design of base frame.

A modular design approach has been adopted to facilitate maintenance, transport, and subsystem replacement processes. The central frame is configured to house critical avionics systems, power electronics, and mission payloads, providing quick access during testing and competition operations.

The current airframe design was used during the 2025 racing season and has been verified to successfully meet weight, volume, and autonomous flight requirements. Accordingly,

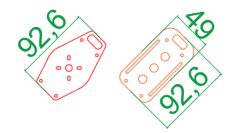

Fig. 4. Airframe Motor Mount

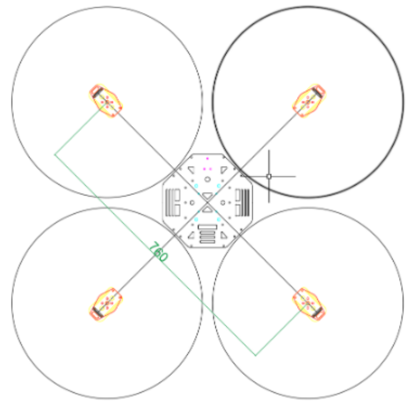

Fig. 5. Airframe Top View

rather than completely redesigning the platform during the 2026 design process, the focus has been on optimizing it at the subsystem level while retaining the existing structure.

*2) **Propulsion**:* The UAV's maximum takeoff weight (MTOW), including all mission equipment and the power system, has been calculated to be approximately 14.3 lbs (6.5 kg). For multi-rotor unmanned aerial vehicles, a minimum thrust-to-weight ratio (T/W) of 2.0 has been targeted to ensure safe flight performance, sufficient maneuverability, and the ability to handle sudden load changes that may occur during a mission. The total required thrust is given in the equation below based on this requirement.

$$T_{required} = 2 * MTOW$$

$$T_{required} = 2 * 6.5kg = 13kg$$

As a result of the motor-propeller matching studies conducted, **T-Motor MN505-S KV380** [?] motors and **T-Motor 18×6.1-inch** [T-M23] carbon fiber propellers were selected. According to the performance data provided by the manufacturer, each motor-propeller set can generate a maximum thrust of approximately 7.7 lbs (3.5 kg). Accordingly, the system's total thrust capacity was calculated as shown in the equation.

$$T_{total} = 4 * 3.5kg = 14kg$$

The system's thrust-to-weight ratio was calculated using the total thrust value obtained.

$$\frac{T}{W} = \frac{T_{total}}{MTOW}$$

$$\frac{T}{W} = \frac{14}{6.5} = 2.15$$

The calculated thrust-to-weight ratio of 2.15 exceeds the design target of 2.0, indicating that the system has sufficient performance reserves for takeoff, climb, position holding in wind, and payload transport operations. This result confirms that the selected propulsion system is capable of meeting the SUAS 2026 mission requirements.

*3) **Power**:* When selecting a power source for the drone, both LiPo and Li-ion batteries were evaluated. To score 75 points for battery capacity, each battery pack must have a maximum capacity of 100 Wh. To achieve a long flight time, the system requires 16,000 mAh 6S battery. In this case, four lithium-polymer battery packs, each rated at 6S 4,000 mAh, were used. The power distribution board connected to the main battery supplies power to the motors, the Pixhawk, and the camera. Power for the remaining components, including the Raspberry Pi, Bullet AC, and the landing system, is supplied by a separate 3S lithium-ion pack. This separation is intended to isolate the mission computer from current fluctuations in the motor circuit.

B. Mission System

*1) **Image Acquisition**:* The video stream from the Siyi A8 Mini [SIY23] camera is routed to the Raspberry Pi throughout the flight. When the desired location is reached, a frame is captured from this stream and sent to the ground station as shwon in Fig. 6. The transmitted frame contains metadata such as location and time.

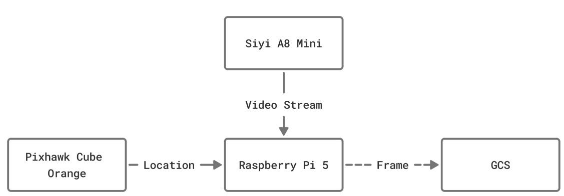

Fig. 6. Image Acquisition

*2) **Target Detection**:* The main task of this system, illustrated in Fig. 12, is to detect people and tents in drone-captured photos and calculate their locations. The obtained location data is then sent back to the drone to facilitate payload delivery. The artificial intelligence model used to detect objects is a specially trained RF-DETR [RRP+26]. It was selected because, based on online benchmarks and our test results (see Fig. 18), it demonstrated superior detection performance compared to YOLO [JQL+26].

The target location is estimated from its image coordinates by projecting the detected pixel onto the ground plane using the drone altitude and camera parameters.

The angular displacement of the target from the image center is calculated as

$$\theta_x = (p_x - c_x)\frac{F_h}{W}$$

$$\theta_y = (p_y - c_y)\frac{F_v}{H}$$

where (p_x) and (p_y) are the target pixel coordinates, (c_x) and (c_y) are the image center coordinates, (F_h) and (F_v) are the horizontal and vertical field of view, and (W) and (H) are the image width and height.

Assuming a nadir-facing camera and a flat ground surface, the target position in the camera coordinate system is obtained by

$$x_c = h\tan(\theta_x),$$

$$y_c = -h\tan(\theta_y),$$

where (h) is the drone altitude.

The camera-frame coordinates are transformed into the world coordinate system using the drone yaw angle (ψ):

$$\begin{bmatrix}\cos\psi & -\sin\psi\ \sin\psi & \cos\psi\end{bmatrix}\begin{bmatrix}x_c\ y_c\end{bmatrix}$$

The horizontal distance between the drone and the target is then calculated as

$$d = \sqrt{x_w^2 + y_w^2},$$

and the bearing angle is determined by

$$\beta = \operatorname{atan2}(x_w, y_w).$$

Finally, using the drone's GPS coordinates, the computed distance (d), and bearing (β), a geodesic forward calculation is performed to estimate the target's geographic coordinates.

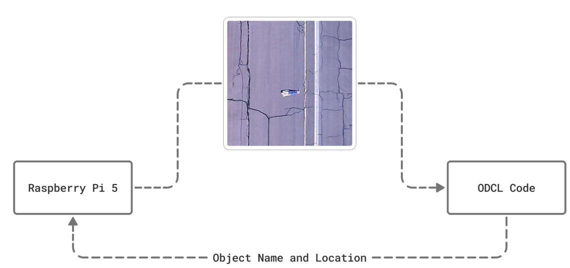

Fig. 7. Target Detection

*3) **Delivery**:* Once the target detection system determines the locations of the objects, the delivery system is activated to navigate the drone to the coordinates and trigger the release sequence. As illustrated in Fig. 8, the delivery mechanism consists of two pulleys mounted on a shaft with a centrally positioned servo motor. Rotating the servo to the right releases the pulley on one side, while rotating it to the left releases the opposite pulley. Once released, the pulley unwinds under the weight of the payload. To control and decelerate the descent, a rotary damper is positioned on the shaft between the pulleys, ensuring safe delivery from an altitude of 65.6 feet.

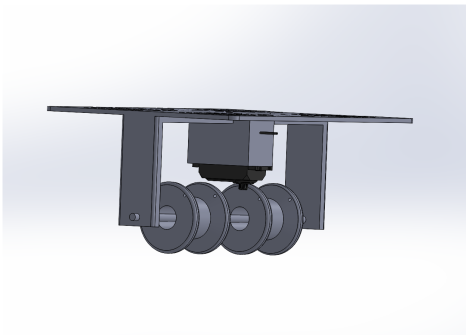

Fig. 8. Delivery Mechanism

*4) **Mapping**:* As illustrated in Fig. 13, the mapping system stores the photos received from the drone and initiates map generation once all images have been transmitted. Map reconstruction is performed using OpenDroneMap (ODM) [Ope23]. To minimize processing time, the number of captured photos must be kept to an optimal minimum. According to our calculations, scanning a 10-acre area from an altitude of 164 feet yields approximately 90 photos. Each photo is captured with a 70% overlap with the previous one, enabling OpenDroneMap to generate the map both efficiently and accurately. Consequently, a full map can be generated from a dataset of 90 photos in approximately 5 minutes.

*5) **Communication**:* The communication system architecture, illustrated in Fig. 9, connects the ground station and the drone via a Wi-Fi link. The drone is equipped with a Ubiquiti Bullet AC module, while the ground station utilizes Ubiquiti LiteBeam AC modules. This setup theoretically enables a 5 GHz connection over distances of up to 6 miles. Signal quality plays a critical role in image transmission, as a weak connection introduces latency and hinders timely mission decision-making. To guarantee high link reliability, a pre-flight spectrum analysis will be conducted to select the most suitable frequency band.

*C. **Safety and Reliability***

Various unforeseen incidents may occur during the competition. This section discusses the strategies we have developed to address these situations.

*1) **Failsafe Strategy**:* Failsafe scenarios are triggered as soon as the system determines that continuing the flight is

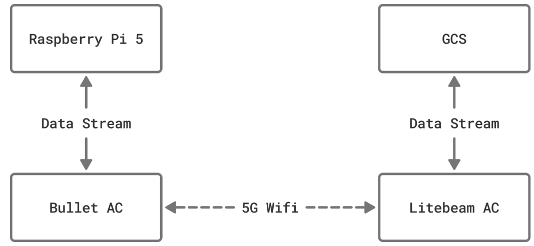

Fig. 9. Communication

unsafe. Examples during a mission include a loss of communication with the RC controller or ground station, or the compass or battery voltage dropping to a critical level. If the system enters failsafe mode, the mission is aborted and the drone switches to RTL mode. The flight will not be repeated until the source of the problem is resolved.

*2) **Wifi Connection Failure Mitigation**:* Various radio devices are used by all teams in the competition area. The large number of devices causes radio interference and disrupts connection stability. For this reason, if the Wi-Fi network, which forms the backbone of the system, cannot be established, the target detection system operating at the ground station is migrated to a Raspberry Pi. To enable the Raspberry Pi to handle this load, the **Hailo 8 AI HAT** module is installed. Since the mapping task is too demanding to be performed on the Raspberry Pi, photos are captured via an SD card as soon as the drone lands, and map processing begins at the ground station.

*3) **Target Detection Failure Mitigation**:* Another contingency plan is for the AI to be unable to detect any objects. If no objects are detected during the first flight, the emergency object-drop procedure is triggered. Delivery is made to the estimated coordinates determined prior to the flight. If the detection issue cannot be resolved after the flight, a third operator descends to the site for detection during the second flight. Since successfully delivering both objects yields a total of 200 points, sacrificing 100 points is a reasonable decision in this scenario.

III. TESTING STRATEGY

*A. **Component Tests***

*1) **Mapping**:* The initial phase of the mapping tests was conducted using a dataset of 63 photographs captured during the 2025 SUAS competition (Fig. 11). The images were taken from an altitude of approximately 164 feet with a 70% overlap. By evaluating various parameters in OpenDroneMap (Table IV), the objective was to identify the optimal configuration that yielded the best map quality in the shortest processing time. Notably, the fast-orthophoto option was enabled by default, as it is known to reduce processing time by up to four times on its own.

feature-quality	sfm-algorithm	orthophoto-resolution	Time (m)	Quality
high	incremental	5	2.47	Perfect
medium	incremental	5	1.44	Bad
low	incremental	5	1.05	Bad
high	incremental	10	2.27	Ok
high	incremental	30	1.29	Ok
high	triangulation	5	2.44	Perfect
high	planar	5	2.43	Perfect

TABLE IV
OPEN DRONE MAP OPTIONS

Table IV lists the parameters believed to have the most significant impact on map quality. As observed, an optimal result could not be achieved in under 2.4 minutes for the 63-photo dataset. To evaluate the effect of dataset size on processing speed, additional performance evaluations were conducted using publicly available datasets (Table V). The benchmark results confirm that processing time scales directly with the number of images.

Photo Count	Time (s)
63	2.47
122	5.33
126	7.02
167	9.16

TABLE V
OPEN DRONE MAP BENCHMARK

2) ***Object Detection:*** Object detection tests were conducted using aerial photographs captured by Türkhan. Small, Medium, and Large variants of the YOLO26 and RF-DETR models were evaluated. As illustrated in Fig. 18, the results demonstrated that RF-DETR consistently detected a higher number of targets than YOLO26, albeit with longer inference times. Consequently, the RF-DETR-Medium model was selected for the mission, as it offers an optimal balance between detection accuracy and processing speed.

B. *Integration Tests*

1) ***Navigation:*** Target alignment tests were conducted within the Gazebo simulation environment, using a red cube to represent a human target. As illustrated in Fig. 10, a test scenario closely mirroring the operational mission profile was executed: the drone takes off, performs a grid scan over the target area, and upon detecting the object, navigates directly to its location to hover briefly before switching to Return to Launch (RTL) mode to conclude the mission.

The results of this test demonstrated that the target detection and flight systems can operate in a coordinated manner.

2) ***Frame and Landing Gear Flexibility Test:*** Structural durability and elasticity tests were conducted to evaluate the system's resistance to physical stress during flight and landing using ANSYS simulations. These analyses encompassed maximum principal elastic strain (Fig. 14), equivalent stress (Fig. 15), directional deformation (Fig. 16), and total deformation (Fig. 17).

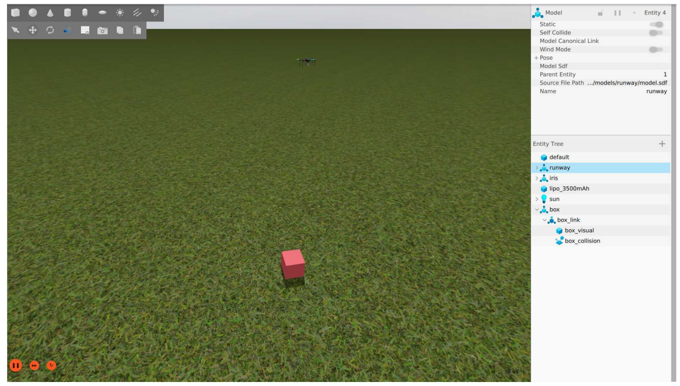

Fig. 10. Gazebo Navigation

REFERENCES

[Hex20] Hex Technology Limited. Cube orange flight controller (pixhawk 2.1). https://docs.cubepilot.org/user-guides/autopilot/the-cube/orange, 2020. Accessed: 2026-04-30.

[Hex21] Hex Technology Limited. Here4 rtk gnss module (u-blox f9p based). https://docs.cubepilot.org/user-guides/here-4-gps, 2021. Accessed: 2026-04-30.

[JQL+26] Glenn Jocher, Jing Qiu, Mengyu Liu, Shuai Lyu, Fatih Cagatay Akyon, and Muhammet Esat Kalfaoglu. Ultralytics yolo26: Unified real-time end-to-end vision models, 2026.

[MAV23] MAVLink Developers. Mavlink micro air vehicle communication protocol. https://mavlink.io/, 2023. Accessed: 2026-04-30.

[Ope23] OpenDroneMap Contributors. Opendronemap: Open source toolkit for processing aerial imagery. https://www.opendronemap.org/, 2023. Accessed: 2026-04-30.

[RRP+26] Isaac Robinson, Peter Robicheaux, Matvei Popov, Deva Ramanan, and Neehar Peri. Rf-detr: Real-time detection transformer. In *International Conference on Learning Representations (ICLR)*, 2026.

[SIY23] SIYI. Siyi a8 mini 4k 8mp ultra hd 6x digital zoom gimbal camera. https://shop.siyi.biz/products/siyi-a8-mini-gimbal-camera, 2023. Accessed: 2026-04-30.

[T-M23] T-Motor. 18x6.1 inch carbon fiber propeller for uav applications. https://store.tmotor.com/product/propeller.html, 2023. Accessed: 2026-04-30.

APPENDIX

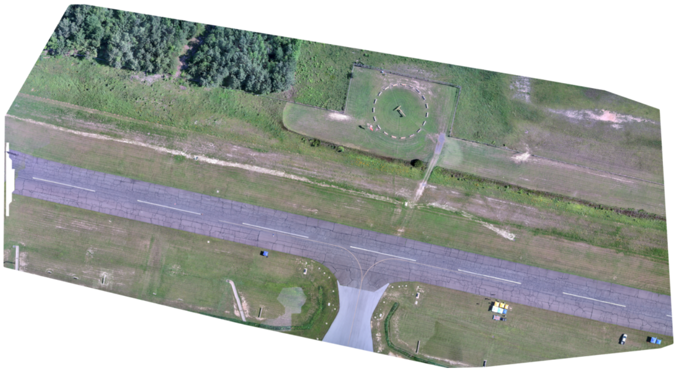

Fig. 11. Suas 2025 Map

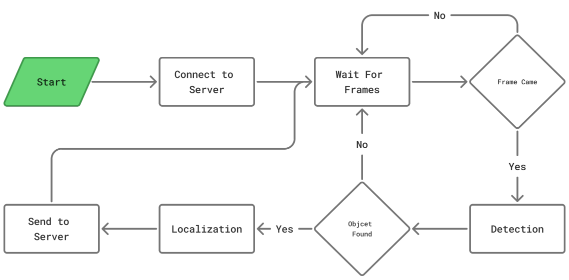

Fig. 12. Target Detection System Flowchart

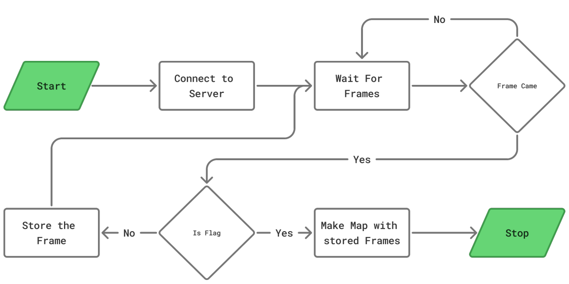

Fig. 13. Mapping System Flowchart

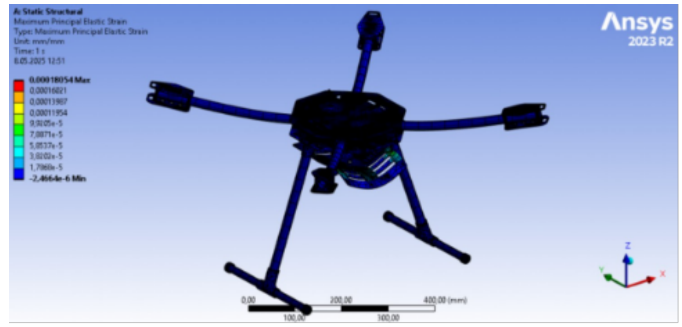

Fig. 14. Maximum Principal Elastic Strain Analysis

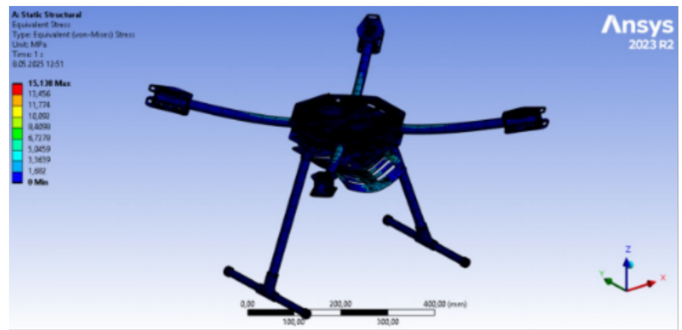

Fig. 15. Equivalent Stress Analysis

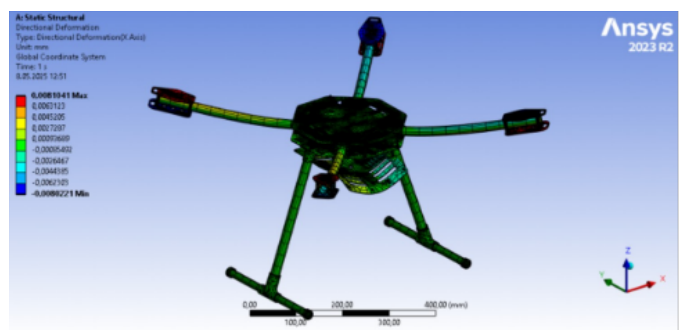

Fig. 16. Directional Deformation Analysis

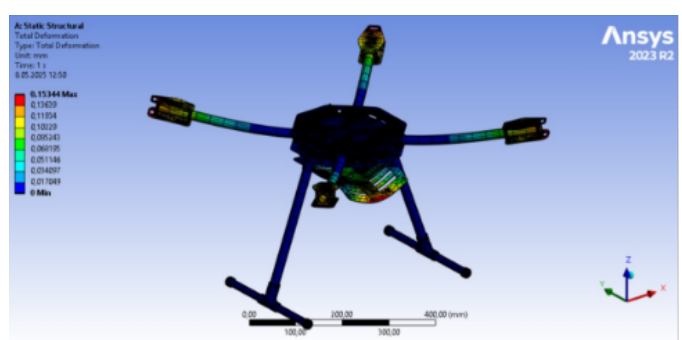

Fig. 17. Total Deformation Analysis

Model	Frame 1	Frame 2	Frame 3	Inference Time
YOLO26s		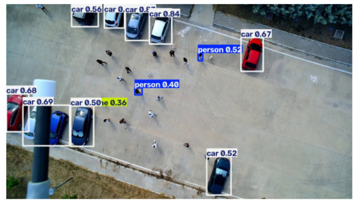	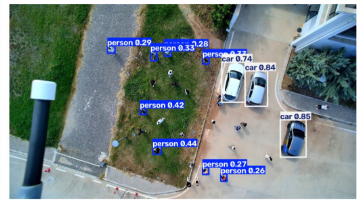	69ms
YOLO26m				114ms
YOLO26l	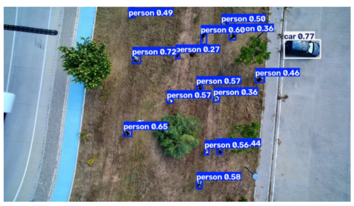		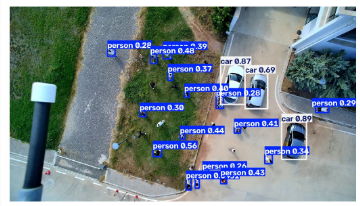	140ms
RF-DETR-S		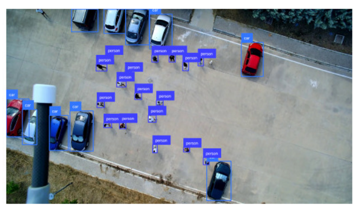		131ms
RF-DETR-M		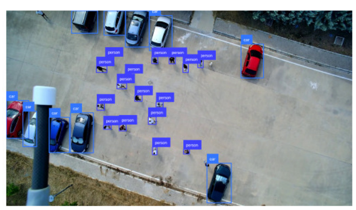		175ms
RF-DETR-L		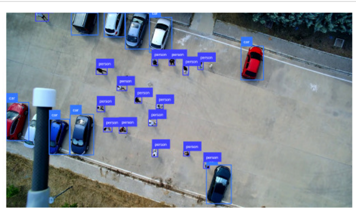		776ms

Fig. 18. Model Tests